J Physiol 589.7 (2011) pp 1627–1642

The Journal of Physiology

The interaction of visual, vestibular and extra-retinal mechanisms in the control of head and gaze during head-free pursuit

Rochelle Ackerley and Graham R. Barnes

Faculty of Life Sciences, University of Manchester, Manchester, UK

Non-technical summary In everyday life, we encounter moving objects and to follow them, we have developed smooth pursuit eye movements. When you rotate your head, the vestibulo-ocular reflex is activated, which generates compensatory smooth eye movements so your eyes remain focussed on the current object of interest. Previous work has shown that you can overcome this reflex to follow a moving object with your eyes and head together, but this normally requires visual feedback. The current study shows that under certain circumstances, for example when you can anticipate the motion of an object, you can use predictive mechanisms in the brain to supplement your pursuit movements to continue to follow the object if it disappears. We demonstrate that you can sample and store brief visual motion to pursue an unseen moving object. Additionally, you can more accurately follow it with your eyes and head together, compared to just using your eyes.

Abstract The ability to co-ordinate the eyes and head when tracking moving objects is important for survival. Tracking with eyes alone is controlled by both visually dependent and extra-retinal mechanisms, the latter sustaining eye movement during target extinction. We investigated how the extra-retinal component develops at the beginning of randomised responses during head-free pursuit and how it interacts with the vestibulo-ocular reflex (VOR). Subjects viewed horizontal step-ramp stimuli which occurred in pairs of identical velocity; velocity was randomised between pairs, ranging from ± 5 to 40 deg s^{-1}. In the first of each pair (short-ramp extinction) the target was visible for only 150 ms. In the second (initial extinction), after a randomised fixation period, the target was extinguished at motion onset, remaining invisible for 750 ms before reappearing for the last 200 ms of motion. Subjects used motion information acquired in the short-ramp extinction presentation to track the target from the start of unseen motion in the initial extinction presentation, using extra-retinal drive to generate smooth gaze and head movements scaled to target velocity. Gaze velocity rose more slowly than when visually driven, but had similar temporal development in head-free and head-fixed conditions. The difference in eye-in-head velocity between head-fixed and head-free conditions was closely related to head velocity throughout its trajectory, implying that extra-retinal drive was responsible for countermanding the VOR in the absence of vision. Thus, the VOR apparently remained active during head-free pursuit with near-unity gain. Evidence also emerged that head movements are not directly controlled by visual input, but by internal estimation mechanisms similar to those controlling gaze.

(Received 20 September 2010; accepted after revision 31 January 2011; first published online 7 February 2011)
Corresponding author R. Ackerley: Faculty of Life Sciences, University of Manchester, Moffat Building, Sackville Street, PO Box 88, Manchester, M60 1QD, UK. Email: rochelle.ackerley@manchester.ac.uk

Abbreviations FEF, frontal eye fields; IE, initial extinction condition; MRE, mid-ramp extinction condition; MST, medial superior temporal cortex; MT, middle temporal cortex; SEF, supplementary eye fields; SRE, short-ramp extinction condition; VOR, vestibular-ocular reflex.

DOI: 10.1113/jphysiol.2010.199471

Introduction

When humans track moving objects with their eyes, smooth pursuit movements are initially driven by visual feedback; subsequently, internal (extra-retinal) mechanisms take over and can sustain the response without vision (Becker & Fuchs, 1985; Bennett & Barnes, 2003). Unexpected target motion normally elicits smooth pursuit responses after 80–100 ms (Carl & Gellman, 1987). Within the next 100 ms, acceleration of the eye is proportional to target velocity (Lisberger & Westbrook, 1985), indicating that target velocity information has been extracted within the brief initial period and used to scale the response. If the target disappears after the first 100–200 ms, internal drive mechanisms sustain eye velocity, without visual input, at a level scaled to target velocity (Barnes & Collins, 2008*a*), indicating that the pursuit system is able to sample and store the initial target velocity estimate. Recent experiments reveal that the internally driven component has much slower temporal development than the visually driven component and is probably generated by mechanisms that also produce slowly accelerating anticipatory movements that occur prior to predictable target motion (Barnes & Collins, 2008*b*).

In everyday situations, pursuit is more likely to be conducted with head and eyes together than with the head fixed. Head rotation stimulates the vestibulo-ocular reflex (VOR), generating compensatory smooth eye movements that are counterproductive to the goal of target pursuit and need to be countermanded. In humans, there is a close association between pursuit and the mechanisms responsible for visual suppression of the VOR (Barnes *et al.* 1978; Barnes, 1993), but how the VOR might interact with the separate retinal and extra-retinal components of pursuit is unknown. Cognitive influences, such as imagining a head-fixed target in darkness, are known to modify VOR gain (Barr *et al.* 1976), although the level of suppression is generally less than achieved with visual input (Barnes & Eason, 1988). Evidence also indicates that vestibular efferent signals may be partially suppressed by extra-retinal mechanisms during active head movements (Roy & Cullen, 2004). The aim of the present study was to investigate the interaction between the extra-retinal component of pursuit and the VOR, using protocols in which the target was temporarily extinguished, thus isolating the extra-retinal component of pursuit.

Method

A total of eight consenting, healthy subjects (four male) participated in the present study, which conformed to local ethical approval (University of Manchester) and was performed in accordance with the *Declaration of Helsinki*. Of these subjects, two were the authors, two had some experience of other eye movement experiments, but four were naïve. No prior training was given other than a brief demonstration run to familiarise the subjects with the experimental conditions. Subjects were seated and instructed to follow a small (<1 deg diameter) circular visual target either with the eyes only or with eyes and head together. The target was formed by projection of an image of an LED onto a semi-circular screen in front of the subject in a darkened room; target motion was controlled by a computer program via a mirror galvanometer. The use of an LED target allowed rapid switching and hence precise timing of target visibility. Eye movements were recorded using an infra-red limbus tracking system (Skalar Iris) attached to a lightweight helmet. Rotational (yaw) head movements were transduced by a continuous turn potentiometer attached to the helmet. The helmet was coupled to an impression dental bite bar, which ensured that the eye movement recorders and the helmet were rigidly coupled to the subject's head.

Experiments were conducted in which the subject's expectation of target motion was manipulated by extinguishing the target during different parts of each trial. The conditions are summarised in Fig. 1, which shows the displacement of the target motion over time and the periods where the target is not illuminated. There were three different test conditions: (1) in the Control condition the target was continuously illuminated and moved for 950 ms (Fig. 1*A*); subjects were simply instructed to follow the target motion; (2) In the mid-ramp extinction (MRE) condition the target again moved for 950 ms. It was visible for the first 150 ms, but was then extinguished for 600 ms, during which time the unseen target continued on its trajectory; it subsequently reappeared and continued to move along the same trajectory for a further 200 ms (Fig. 1*B*). Thus, in the MRE condition subjects had an expectation that the target would move briefly, disappear, then reappear later. Subjects were instructed to attempt to continue pursuit during the extinction; (3) In the short-ramp extinction–initial extinction (SRE–IE) condition trials were presented in matched-velocity pairs but with different parts of the trajectory illuminated in each component of the pair. As in the Control and MRE conditions, target motion in each pair lasted 950 ms. In the first of each pair, target motion was only visible for the first 150 ms; thereafter it continued on its unseen trajectory for a further 800 ms (SRE; Fig. 1*C*). The target then moved back to centre and was illuminated for a randomised period of 1–3 s. In the second of each pair, extinction of the stationary target coincided with the start of target motion, but the target remained invisible for 750 ms (Fig. 1*D*). Target extinction thus signalled the start of unseen motion, which the subject knew would be identical to that in the previous SRE trial. In this second matched-velocity ramp (IE condition), only the final 200 ms of motion was seen, although subjects

were encouraged to make predictive movements to pursue the unseen target. This stimulus pairing thus allowed a dissociation of the visually evoked response to brief motion in the first presentation of the pair (SRE) from the internally driven response to remembered motion in the second presentation of the pair (IE), where no direct visual input was available until 750 ms after motion onset. This was similar to splitting the MRE condition into two parts, but with an intervening period of fixation.

In each condition the stimulus consisted of step-ramp visual target motion, in which a stationary, central target made a small step either left or right, then moved in the opposite direction to cross the central point after 200 ms of motion (Rashbass, 1961). Responses were examined in two protocols, with the head fixed (immobilised by a chin rest and side head clamps) and with the head free to rotate. In head-fixed trials, target velocities of 5, 10, 15 and 20 deg s^{-1} were used, whereas in head-free trials, higher target velocities of 10, 20, 30 and 40 deg s^{-1} were used that more naturally elicited head movement. The subject was informed of the test condition (Control, MRE or SRE–IE pairs) prior to the start of each block. Individual trials in a condition block were randomised for the direction of movement and speed of the target, making the target trajectory highly unpredictable; the condition blocks were presented in a balanced, randomised order. Twelve repeats were presented at each target speed for each subject, resulting in blocks containing a total of 48 step-ramp stimuli. Each block of trials was preceded by a calibration of the eye movement recorders in which subjects were instructed to maintain the head stationary whilst following a sinusoidal target motion (0.4 Hz, $\pm$20 deg s^{-1}) with the eyes alone. In the head-free conditions, head rotation was also recorded during the calibration so that any small inadvertent head movement could be accounted for. During the experiment, subjects were instructed to pursue the target whilst it was visible and to attempt to track the target along its expected trajectory during target extinction.

The analogue eye and head displacement data were low-pass filtered at 80 Hz and stored off-line after digitisation at 200 Hz. In head-fixed conditions, the left eye displacement data were used; in the head-free conditions, the left eye and the head displacement signals were summated to give gaze displacement data, which were then digitally differentiated to obtain gaze velocity.

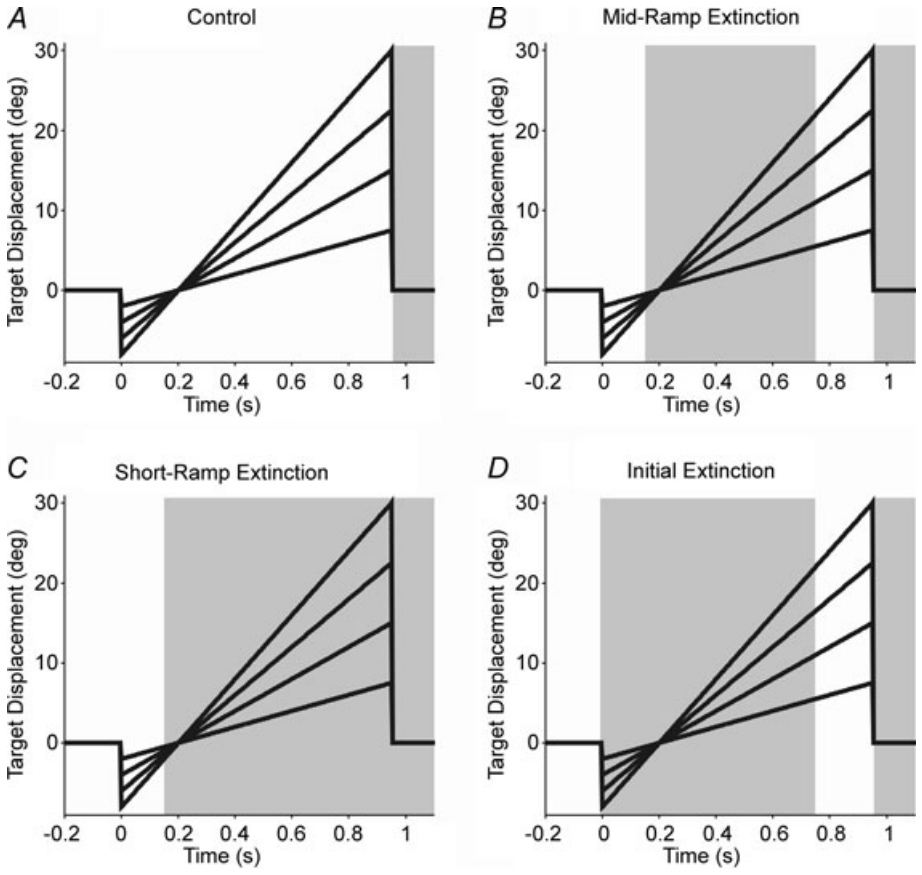

Figure 1. Target displacement and illumination over the conditions
Head-free target displacement is shown (10, 20, 30 and 40 deg s^{-1}); for head-fixed displacement (5, 10, 15 and 20 deg s^{-1}), divide the *y* axis values by two. Shading indicates periods of target extinction.

Before the main analysis, saccadic movements and blinks were removed using an interactive graphics procedure based on gaze acceleration (see Bennett & Barnes, 2004 for details). Linear interpolation was used to fill the gaps after saccade removal and the resultant smooth gaze velocity movements were filtered with a 30 Hz zero-phase digital low-pass filter. Head and target velocity information were derived by digital differentiation of head and target displacement data, respectively. In further analyses, responses were averaged over repeats and also over left- and right-going targets, since no significant directional disparity was found.

The latencies for smooth gaze movement and head movement were determined by interactive marking and recording of the point of onset. The position at the end of the extinction period was recorded for gaze, head and eye movements. Similarly, gaze, head and eye velocity at the end of the extinction period and at other time points during target extinction were also calculated and compared between different test conditions and target velocities. Statistical comparisons of gaze and head velocities were made with repeated-measures ANOVA tests using SPSS software, with planned contrasts where relevant. Mauchly tests were used to test sphericity within and between factors; if sphericity was violated, a Greenhouse–Geisser correction was used to calculate the P value. Additionally in this analysis, linear regressions were used to explore the relationship between head-fixed and head-free pursuit dynamics. The results from the head-fixed and head-free parts of the experiment were compared. Six of the subjects completed both the head-fixed and head-free protocols, allowing direct comparisons in gaze velocity at matched target velocities of 10 and 20 deg s^{-1}.

Results

General observations

Comparing the response trajectories in Fig. 2 (eye; head-fixed) and Fig. 3 (gaze; head-free), it is clear that they were dependent on the amount of visual motion information available. In Control conditions, where the whole target trajectory was seen, eye and gaze pursuit closely followed target displacement and velocity, as expected when visual feedback can correct tracking errors (Figs 2*A* and 3*A*, respectively). In the MRE condition, eye and gaze pursuit were sustained throughout the target extinction (Figs 2*B* and 3*B*, respectively), attaining fairly constant velocity, though this was less than the target for higher target velocities. In comparison, in the SRE condition, eye and gaze velocity reached an initial peak, that increased with target velocity, but this was not sustained and decreased over the following 600 ms. Furthermore, in the head-free SRE trials (Fig. 3*C*), gaze velocity was maintained for longer than in the head-fixed SRE trials (Fig. 2*C*), where a sharper decrease in eye velocity occurred. The contrast between the MRE and SRE conditions shows the effect of cognitive processes (i.e. the expectation of target reappearance) on the ability to sustain extra-retinal pursuit.

In the IE condition, subjects were able to use the brief visual motion from the preceding SRE trial to generate a pursuit response in the complete absence of vision. In response to the extinction of the fixation cue ('go cue'), a steady build-up of gaze velocity occurred throughout extinction, driven by internal mechanisms alone; there was no initial open-loop, fast acceleration to a visual target. The slowly developing gaze velocity was qualitatively similar in head-fixed and head-free protocols and, in both conditions, eye or gaze velocity increased with the velocity of the unseen target (see Figs 2*D* and 3*D*, respectively). In all head-free test conditions head responses had quite similar bell-shaped velocity trajectories that were scaled to target velocity (Fig. 3). These head trajectories, however, contrasted with the widely different gaze velocity trajectories observed in the different test conditions.

Table 1. Mean onset latency (ms) ± SD of eye, head and gaze velocity in response to each of the test conditions

Test condition	Eye (fixed)	Gaze (free)	Head (free)
Control	129.4 ± 16.4	141.9 ± 12.7	237.1 ± 19.0
Mid ramp extinction	134.9 ± 9.9	146.8 ± 13.2	227.2 ± 19.1
Short ramp extinction	129.8 ± 14.0	142.3 ± 15.8	202.7 ± 19.1
Initial extinction	208.6 ± 58.1	193.0 ± 44.9	206.2 ± 53.0

Response latency

Eye, gaze and head velocity onset latencies were calculated with respect to target motion onset, whether the target was visibly moving (Control, MRE and SRE conditions) or not (IE condition). Mean eye latencies (± SD) are shown in Table 1. Repeated-measures ANOVA were conducted for the eye, gaze and head data separately, with the four conditions and four target velocities as levels in each of the factors. The analysis revealed a significant difference in onset latency between conditions in both the head-fixed ($F = 10.29$, $P < 0.05$) and head-free protocols ($F = 7.27$, $P < 0.05$). Simple contrasts, using the Control as a baseline, indicated that the onset latency in the IE condition was significantly delayed compared to the Control (head fixed: $F = 9.01$, head free: $F = 6.07$, $P < 0.05$). No significant differences were found in the onset latencies between any of the conditions for the head movement onset, indicating that, unlike gaze onset, head movement onset was not affected by the presence or absence of initial visual input.

A comparison was made between eye movement onset latencies in the head-fixed and head-free protocols for the matched target velocities of 10 and 20 deg s^{-1}: no significant difference was found. A comparison was also made in the head-free protocol between onset latencies of the gaze and head responses. This revealed a significant longer latency for the head than for gaze ($F = 33.70$, $P < 0.001$) in the conditions where there was initial visual input (Control, MRE and SRE). However, in the IE condition with no initial visual input, there was no significant difference between the onset of the gaze and head responses. Thus, non-visual mechanisms initiated gaze and head movement concurrently in the same direction.

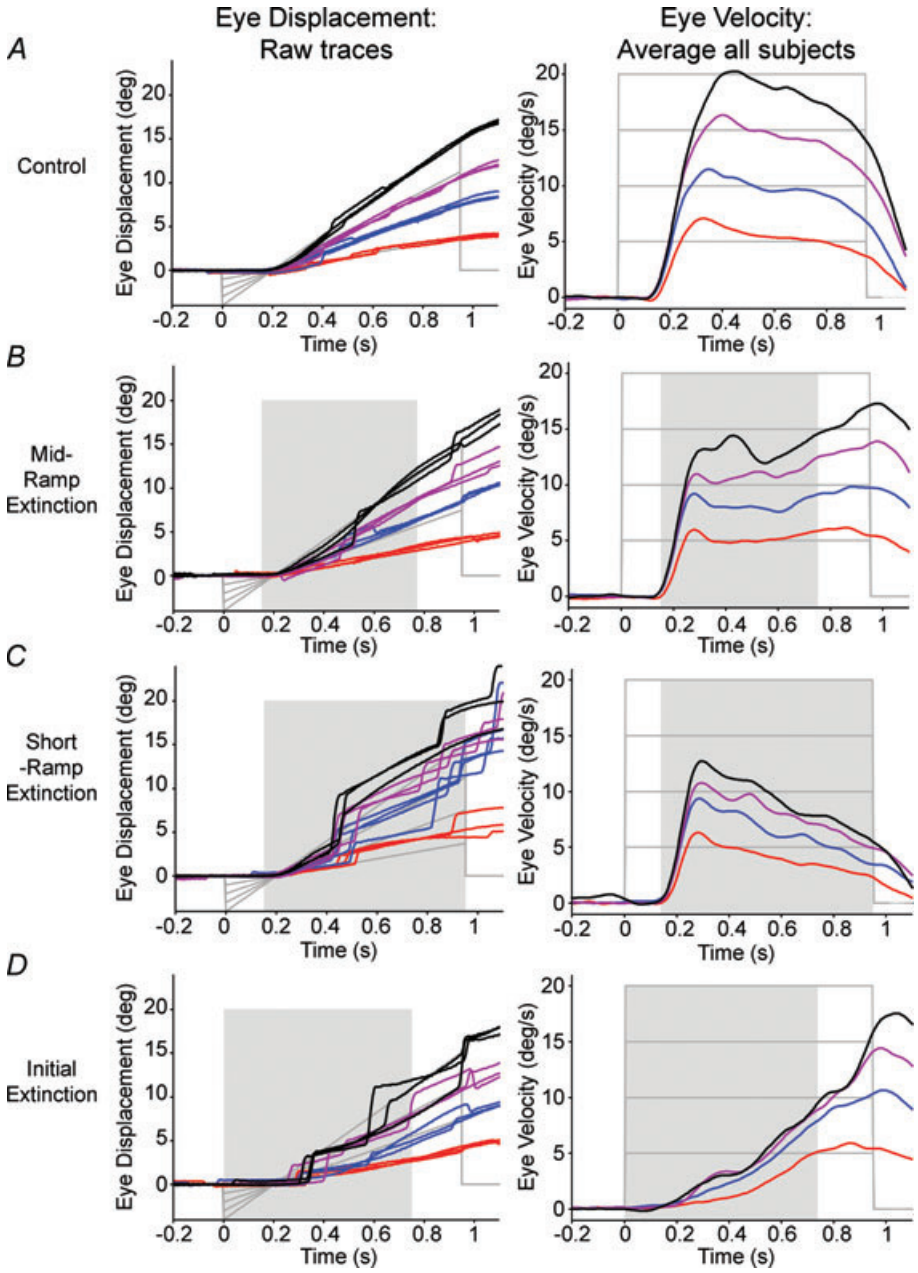

Figure 2. Head-fixed eye responses to all conditions over target velocities of 5–20 deg s^{-1}
Raw eye displacement traces from subject 1 ($n = 3$ per target velocity; left column) and average eye velocity from all subjects (right column), over all the conditions. In general, eye displacement over the different conditions was well-scaled to target displacement. In comparison, eye velocity varied between conditions, although was nevertheless scaled to target velocity. Key to target velocity: red, 5 deg s^{-1}; blue, 10 deg s^{-1}; purple, 15 deg s^{-1}; black, 20 deg s^{-1}. Target displacement and velocity are shown in grey lines. Shading indicates periods of target extinction during motion.

Eye/gaze displacement

Gaze displacement was well-scaled to target velocity across all motion conditions, especially at the lower target velocities, whether the head was fixed or free to rotate (Figs 2 and 3, first columns). The displacement of gaze was measured at 750 ms from the onset of target motion as this corresponded to the end of target extinction in the MRE and IE conditions. This was the latest time at which responses could be contrasted across conditions to assess the contribution of internally driven mechanisms during extra-retinal pursuit. Significant differences were found

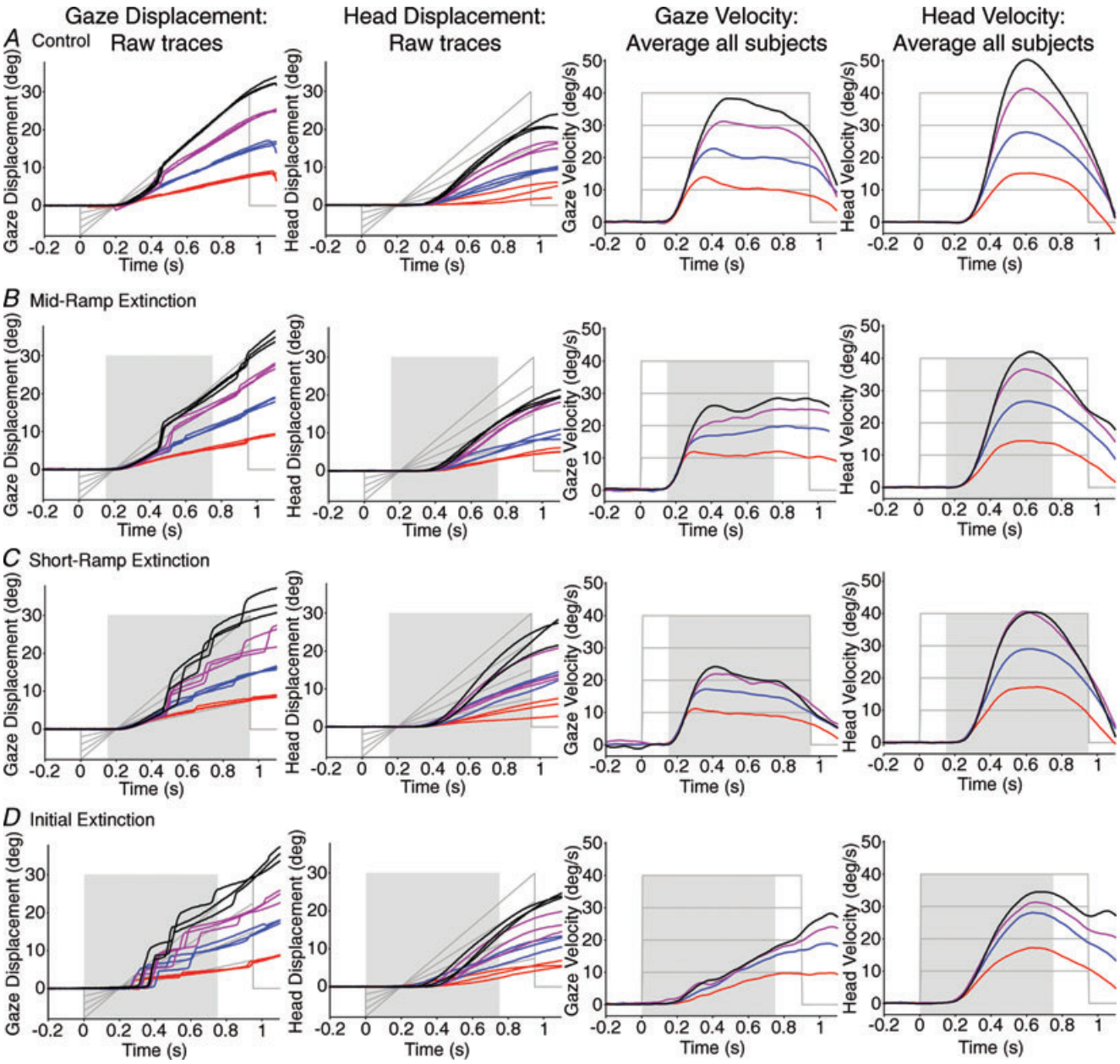

Figure 3. Head-free gaze and head responses to all conditions over target velocities of 10–40 deg s^{-1}
Raw gaze displacement traces from subject 3 ($n = 3$ per target velocity; first column) and matched head displacement, over all conditions (second column); average gaze velocity from all subjects (third column) and average head velocity (fourth column), over all conditions. Gaze displacement was accurate to target displacement, but head displacement was typically lower than target displacement. Gaze and head velocity responses were scaled to target velocity. Gaze velocity exhibited different response trajectories for the different conditions, but head velocity trajectories remained similar for all conditions, at least for the first 750 ms of each trial. Key to target velocity: red, 10 deg s^{-1}; blue, 20 deg s^{-1}; purple, 30 deg s^{-1}; black, 40 deg s^{-1}. Grey lines denote target displacement and velocity. Shading indicates periods of target extinction during motion.

between increasing target velocities for end-extinction gaze displacement in both the head-fixed and head-free protocols (see Fig. 4*A* and *B* and Table 2 – displacement for eye/gaze over target velocity). This indicated that all responses were scaled to target velocity, even when the target was not visible. The visual motion available to drive pursuit differed between test conditions, but only in the head-fixed results was there a significant main effect of test condition (Table 2 – test condition for eye displacement).

Eye/gaze velocity

Although gaze displacement was well-matched to target displacement, gaze velocity fell short of target velocity during extra-retinal pursuit. Figs 2*A* (right column; head fixed) and 3*A* (third column; head free) highlight how direct visual motion provided feedback to guide smooth pursuit in the Control condition. When this continuous visual feedback was removed in the extinction conditions, pursuit was less accurate and the velocity of the responses decreased, particularly at higher target velocities (Figs 2*B–D* and 3*B–C*). Response velocity was compared at the time equivalent to the end of target extinction (750 ms after motion onset); the results are shown in Fig. 4*C* and *D* over all conditions and target velocities. End-extinction eye and gaze velocity increased significantly with each level of target velocity both when the head was fixed and free to rotate (Table 2 – velocity for eye/gaze over target velocity). Comparing eye/gaze velocity over the different conditions, significant differences were also found for both the head-fixed and head-free protocols (Table 2 – velocity for eye/gaze over test condition). Specifically, the SRE and IE conditions were significantly lower in eye/gaze velocity compared to the Control.

Head movement

Figure 3 shows examples of raw head displacement (second column) and the average head velocity (last column) over the different conditions. It is evident that head displacement formed a large proportion of total gaze displacement (cf. gaze and head displacement in Fig. 3*A* and *B* respectively), but head displacement was always less than gaze. The calculation of head displacement at the time corresponding to end-extinction provides a clear indication of the parsing of gaze between head and eye (Fig. 4*B*). ANOVA revealed a significant effect of target velocity on end-extinction head displacement

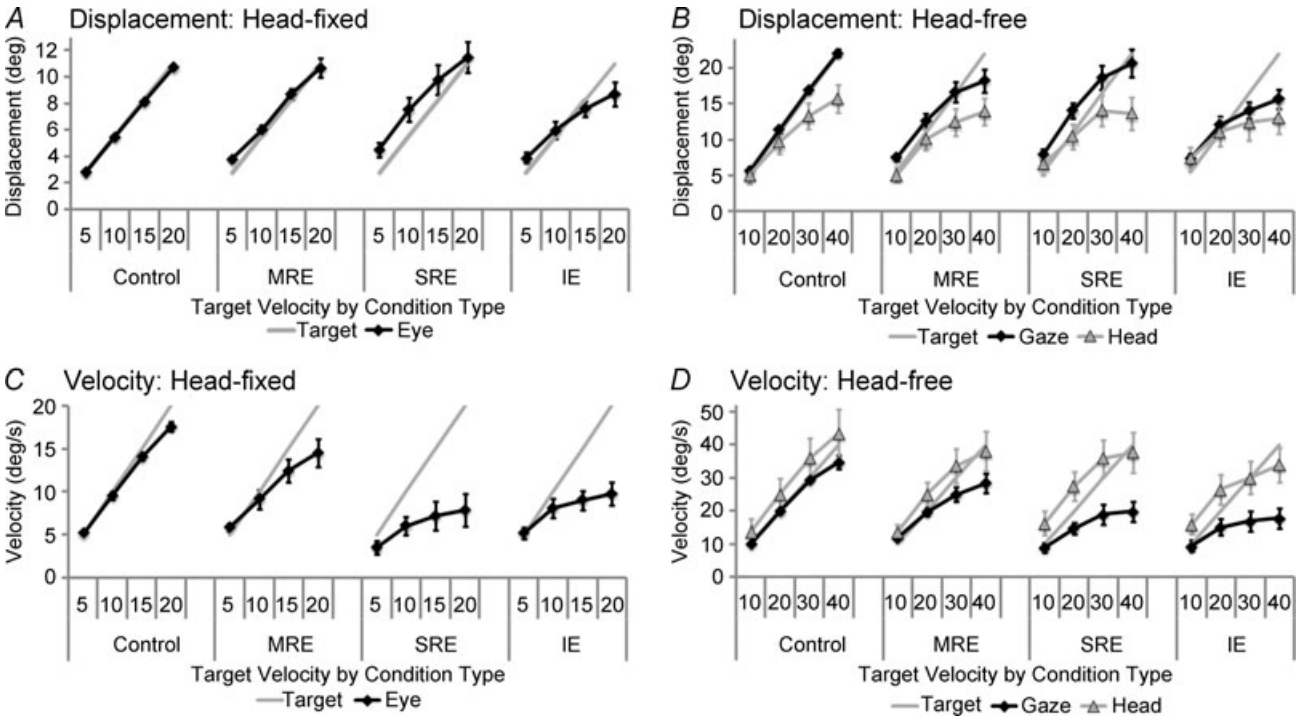

Figure 4. Displacement and velocity values at 750 ms (end-extinction equivalent time) for head-fixed and head-free protocols
The figure shows average responses from all subjects for eye (head-fixed, left graphs), gaze (head-free, right graphs, squares) and head (right graphs, triangles). In the conditions where visual feedback is removed, eye and gaze displacement (*A* and *B*, respectively) were better matched to target displacement than eye and gaze velocity were to target velocity (*C* and *D*, respectively). The head-free responses show the head displacement and velocity, where the head contributes a substantial amount to the overall gaze displacement and head velocity is similar whether there is visual motion or not. Error bars denote ± 1 SEM.

Table 2. Statistical analyses of the head-fixed eye and head-free gaze and head data over target velocity and test condition

	Eye (fixed)	Gaze (free)	Head (free)
Displacement			
Target velocity	195.52**	99.57**	47.00**
Test condition	5.56*	*n.s*	*n.s*
Velocity			
Target velocity	72.85**	64.06**	39.25**
Test condition	14.76**	11.94**	*n.s.*

The table shows *F* values from repeated-measures ANOVA on end-extinction displacement and velocity data, for the eye, gaze and head using separate tests. For target velocity, repeated contrasts showed significant increases ($P < 0.05$) for all the measures (eye, gaze and head displacement and velocity) with the progression from one level of target velocity to the next. For test condition, simple contrasts were used to compare the IE, SRE and MRE conditions to the Control. The only significant differences ($P < 0.01$) found were for the eye and gaze velocity responses comparing the Control to the SRE and the IE conditions. $^{*}P < 0.01$, $^{**}P < 0.001$.

(Table 2); the head movements were scaled to target velocity. Similarly, end-extinction head velocity (Fig. 4*D*) also increased significantly with target velocity (Table 2). There was no significant effect of test condition on end-extinction head displacement or velocity (Table 2) and a more detailed comparison of head velocity at 100 ms intervals over the first 700 ms also revealed no significant difference between test conditions. Thus, the brief presentation of visual motion information at the beginning of the trial in the extinction conditions (and stored motion in the IE condition) was used to direct and scale head movements. In contrast to gaze velocity (described above), head velocity was remarkably similar across test conditions and, in particular, was not significantly influenced by the presence or absence of a concurrent visual stimulus.

Comparison of head-free and head-fixed responses

It is evident from results so far that the ability to accurately pursue a moving target is affected by target visibility and the expectation of target appearance. For both head-fixed and head-free protocols, gaze velocity was significantly modified by the test condition, whereas the displacement responses were less influenced by this factor. To investigate further the internal mechanisms driving smooth pursuit, head-fixed eye velocity was directly compared to head-free gaze velocity in the same six subjects for the target velocities of 10 and 20 deg s^{-1}. As expected, in the Control condition no significant differences were found between head-fixed and head-free responses, where continuous visual feedback was present; gaze velocity was well matched to target velocity for both. Comparison of the responses in the paired SRE–IE condition, however, yielded a very different result. Figure 5*A* and *B* clearly demonstrate that throughout the responses, for both SRE and IE conditions, head-free gaze velocity was consistently higher than the equivalent head-fixed eye velocity (compare continuous *vs.* dashed lines). A similar effect was also observed for the MRE condition, where gaze velocity was higher than eye velocity for matched-target velocity trials (not shown here for clarity). The effect for the SRE and IE conditions was quantified by calculating gaze velocity at the time equivalent to the end of target extinction, i.e. 750 ms after target motion onset (Fig. 5*E*). There was a significant increase in end-extinction gaze velocity between the head-fixed and head-free conditions ($F = 18.07$, $P < 0.01$); a significant increase in gaze velocity was also found as the target velocity increased from 10 to 20 deg s^{-1} ($F = 27.63$, $P < 0.01$). However, there was no significant difference between the SRE and IE conditions at the end-extinction time. Essentially, gaze velocity in the IE condition rose steadily during extinction to closely match the slowly decaying velocity in the SRE condition at the time equivalent to end-extinction.

In contrast to gaze velocity, the end-extinction gaze displacement (Fig. 5*D*) showed no significant differences between head-fixed and head-free conditions or between the SRE and IE conditions. However, end-extinction gaze displacement increased significantly with increasing target velocity from 10 to 20 deg s^{-1} ($F = 578.16$, $P < 0.001$).

Modelling the data

The origins of the differences revealed in Fig. 5 will now be explored by considering the responses of a model developed to represent the likely underlying processing. The model (Fig. 6) has been developed as an extension of one presented previously to explain findings during head-fixed pursuit (Barnes & Collins, 2008*b*). In common with other pursuit models (e.g. Robinson *et al.* 1986), it is assumed that visual feedback mechanisms are supplemented by internal efference copy feedback. However, in this model, in order to explain the responses to the SRE–IE pairs, efference copy feedback is comprised of two components: (i) a direct pathway used during the SRE component and (ii) an indirect pathway that contains a specific memory of prior motion stimuli which is assumed to be used in the IE component. Note that, unlike previous models, the input to the efference copy pathway is derived from an explicit internal reconstruction of target velocity (T') that is not part of the direct pursuit drive. This feature was introduced to account for the ability to store motion information even when passively viewing, rather than actively pursuing, the moving target (Barnes *et al.* 1997, 2000; Burke & Barnes, 2008). The incoming signal (T') is captured by the sample and hold module

(S/H) within the first 150 ms and used to generate the extra-retinal pursuit component with gain β and dynamics determined by $F'(s)$. An important additional component of the model is the representation of the VOR dynamics ($V(s)$), which generate eye-in-head movements that are compensatory to head rotation.

We will attempt to identify salient components giving rise to the observed differences between head-fixed and head-free conditions by first examining the responses to the IE protocol, in which there was no initial visual feedback for the initial 750 ms of target motion. Without visual input the equation governing control of eye-in-head velocity (E) is then given by:

$$E = -V(s) \cdot H + \beta \cdot F'(s) \cdot T' \quad (1)$$

where H is head velocity and s is the Laplace operator.

The extra-retinal component ($\beta.F'(s).T'$) of eqn (1) represents the efference copy input derived from the storage of target motion information in the preceding SRE presentation; for the present, it is assumed that this component is identical in head-fixed and head-free conditions. The relationship between eye velocity in the head-free condition (E_{FR}) and the head-fixed condition (E_{FX}) is then given by:

$$E_{FR} - E_{FX} = -V(s) \cdot H \quad (2)$$

Furthermore, since gaze velocity, $G = E + H$:

$$G_{FR} - G_{FX} = (1 - V(s)) \cdot H \quad (3)$$

Figure 7*A* shows superimposed gaze, head and eye-in-head responses in the head-fixed and head-free IE conditions averaged across repeats and across subjects. Head velocity appears to start simultaneously with gaze velocity and, although eye-in-head velocity is oppositely directed to head velocity, its magnitude is somewhat less than the head, so that gaze velocity is in the same direction as the head (and target). By subtracting mean head-fixed eye velocity (E_{FX}) from head-free eye-in-head velocity (E_{FR}) the signal represented by the black dashed trace in Fig. 7*A* can be derived. This eye velocity difference signal has a trajectory similar to an inverted form of head velocity and thus corresponds to the expected output of the VOR, in line with the predictions of eqn (2). Unsurprisingly, when eye velocity difference is plotted

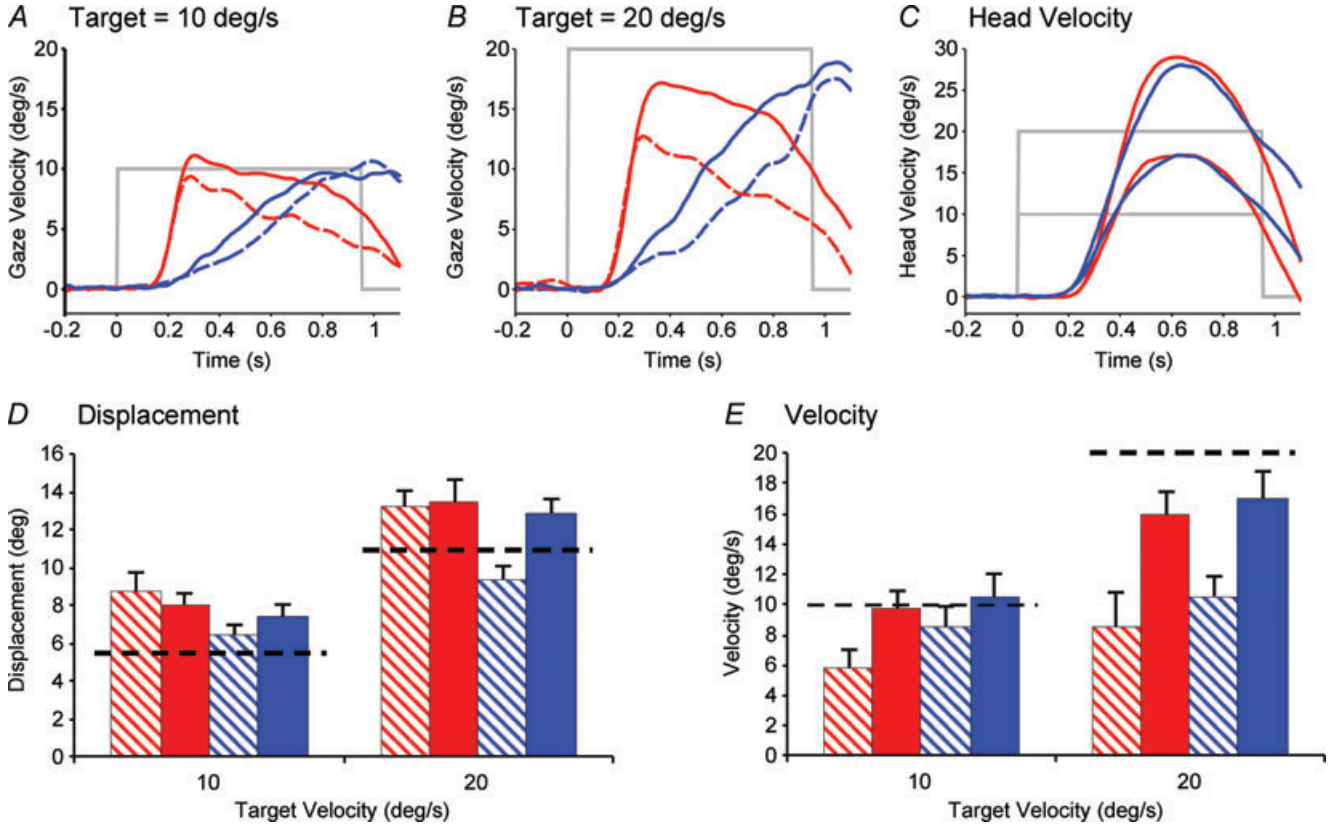

Figure 5. Difference in responses between head-fixed and head-free protocols for SRE and IE pairs
Examples of average gaze velocity profiles for both head-free (continuous lines) and head-fixed (dashed lines) in the SRE (red) and IE (blue) conditions at target velocities of (*A*) 10 deg s^{-1} and (*B*) 20 deg s^{-1}. *C*, head velocity in both conditions at both target velocities. *D*, displacement and *E*, velocity equivalent end-extinction values for head-free (filled) and head-fixed (hatched) for SRE (red) and IE (blue) pairs at target velocities of 10 and 20 deg s^{-1}, +1 SEM. Dashed black line indicates the level of target displacement and velocity at the end of extinction.

against head velocity for the first 750 ms of the response a quasi-linear inverse relationship is revealed (Fig. 7*D*). Assessing head and eye responses in the MRE and SRE conditions is more complex than for the IE condition because of the influence of the brief visual stimulus which evokes the initial rapid rise in gaze velocity. Nevertheless, plotting the eye velocity difference signal for these two conditions in Fig. 7*B* and *C* again reveals that this signal has a trajectory similar to inverted head velocity and when plotted against head velocity (Fig. 7*E* and *F*) an inverse linear relationship is revealed.

Although it would be possible to carry out simple linear regression analyses between the eye velocity difference and head velocity, there are two additional factors that need to be considered. Firstly, although the plots in Fig. 7*D–F* suggest that $V(s)$ may be represented as a simple constant (Kv), it is likely that there is a transmission delay (τ) of ~15 ms (Collewijn & Smeets, 2000) between head velocity and the output of the VOR (i.e. $V(s) = Kv \cdot e^{-\tau s}$). Secondly, it has been assumed so far that the head-fixed data can be compared directly with the head-free data, but this may be unjustified, since there was considerable variance in the responses. A more rigorous approach is to assume that the head-free eye velocity (E_{FR}) is composed of two components, one that has the temporal characteristics of head velocity (gain K_V), and one that has the same temporal characteristics as the head-fixed response, but has variable gain (K_{FX}).

To estimate values of K_V and K_{FX}, multiple regression analysis was conducted with E_{FR} as the dependent variable and E_{FX} and H as independent variables. To estimate the delay (τ) the regression analysis was carried out for delays of 0–50 ms at increments of 5 ms. The delay yielding the highest percentage variance (R^2 value) was then selected; as predicted, optimum solutions were indeed found for delays ranging from 5 to 25 ms in different subjects. Values of K_{FX} and K_V, together with associated R^2 and optimum delay values, are shown in Table 3 for each subject and for all subjects combined. In all cases, the regression analysis gave a highly significant fit to the data, as indicated by the very high values of R^2. The average slope (K_v) for the IE condition was 0.89 at 10 deg s^{-1} and 0.83 at 20 deg s^{-1}. Although individual values of K_{FX} varied quite widely the average values were 1.00 at 10 deg s^{-1} and 0.97 at 20 deg s^{-1}, close to the ideal value of unity. When identical analyses were applied to the SRE and MRE conditions,

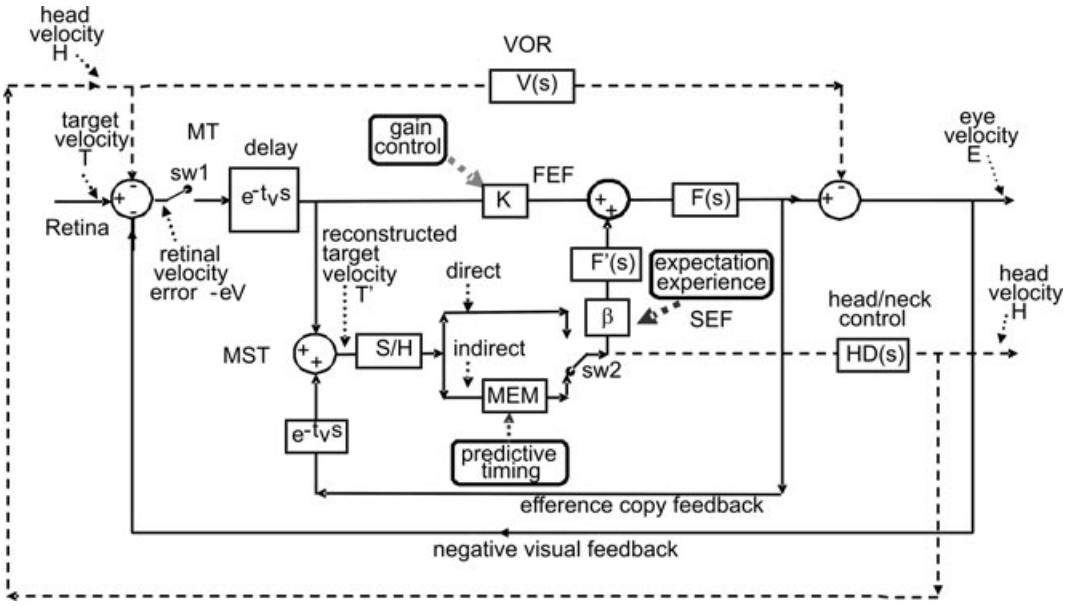

Figure 6. Model of head and eye control during head-free pursuit
The basis of the model is a negative feedback loop in which retinal velocity error is processed by internal dynamics $F(s)$ with variable gain K and a delay of ~80–100 ms. The negative visual feedback is supplemented by extra-retinal input from either a direct or indirect (predictive) loop. The input to both direct and indirect pathways comes from sampling (for ~150 ms) and holding a copy of the reconstructed target velocity signal (T') in module S/H. The direct loop can thus sustain eye velocity even if visual input is withdrawn (i.e. if sw1 is opened). The indirect loop includes a more robust short-term store, MEM, which can hold velocity information over longer periods and during fixation. Both direct and indirect pathways feed out through an expectation-modulated gain control (β) and filter $F'(s)$. Direct and indirect pathways may also control head velocity via head–neck dynamics HD(s). Head movement stimulates the vestibulo-ocular reflex (VOR), which interacts with pursuit pathways in the vestibular nuclei (VN). In a reactive response, S/H output is fed out directly and is also temporarily stored in MEM. In predictive mode, output of MEM is fed out under timing control to form an anticipatory response. For definitions of putative neural substrates (MT, MST, FEF and SEF) see abbreviations.

similar coefficients and R^2 values were obtained (Table 3). The average best fit function for head-free eye-in-head velocity derived from this analysis closely followed the time course of actual eye-in-head velocity for all three test conditions (IE, SRE and MRE in Fig. 7*A*, *B* and *C*, respectively). To conduct this regression analysis we used the Matlab stepwise fit process. This revealed that both coefficients (K_V and K_{FX}) made a significant ($P < 0.001$) contribution to the best fit function in all subjects. For comparison, we also conducted the analysis by assuming that the extra-retinal component played no part during head-free pursuit (i.e. $K_{FX} = 0$). This analysis yielded considerably lower values of the compensatory gain (K_V) and a much poorer fit to the data, as indicated by the R^2 values (Table 3).

In summary, the regression analyses indicate that the best fit between gaze velocity and head velocity throughout the extinction period is obtained when the extra-retinal and retinal components are assumed to have the same temporal development as found in the head-fixed condition. These analyses indicate that the head movement component of gaze (the sum of head and eye) was largely compensated for, since the gain of the compensatory component (K_V) had an overall average of 0.85.

Variability of head and gaze velocity

Although average gaze and head velocity increased with target velocity in all test conditions (IE, SRE and MRE), there was considerable variance in both measures and considerable overlap between the distributions for different target velocities. This suggests that both head and gaze responses made in the absence of vision were estimates based on the initial sampling of motion information. Since both head and gaze were initiated in the absence of visual input we sought evidence for a link between head and gaze velocity, irrespective of target velocity. To make this assessment we calculated gaze velocity and head velocity at fixed times after target onset.

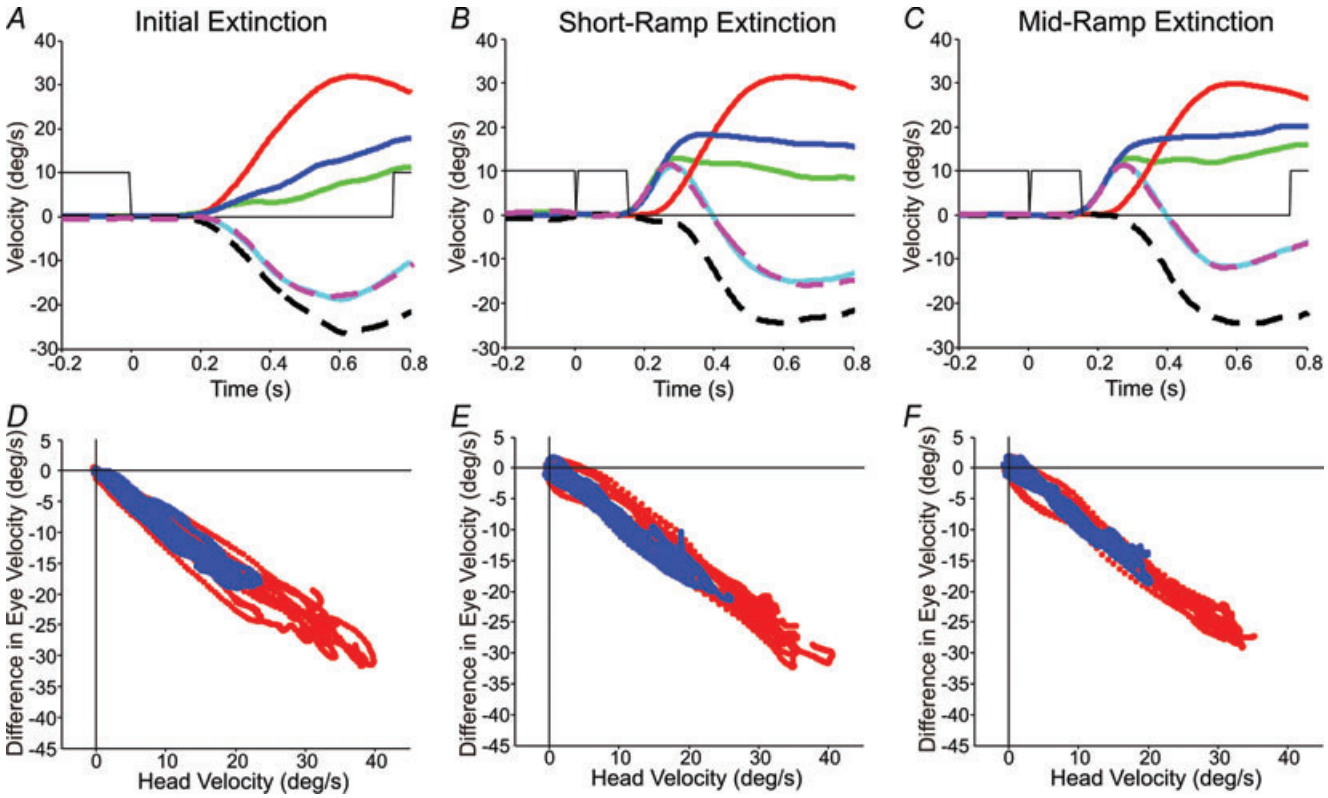

Figure 7. Time course of response development and eye velocity difference plotted as a function of head velocity in extinction conditions
Time course of response development for IE (*A*), SRE (*B*) and MRE (*C*) conditions; traces are as follows: head-free gaze velocity (blue), head-fixed eye velocity (green), head velocity (red), head-free eye-in-head velocity (cyan) and best fit derived from regression analysis (dashed magenta). The black dashed trace represents the eye velocity difference signal (= head-free eye-in-head velocity minus head-fixed eye velocity). Responses are averaged across all subjects and shown at the 20 deg s^{-1} target velocity. Grey lines indicate target illumination. Eye velocity difference plotted as a function of head velocity for averages in IE (*D*), SRE (*E*) and MRE (*F*) conditions. The eye velocity difference (head-free eye-in-head minus head-fixed eye-in-head velocity) as a function of the head velocity is shown for 10 deg s^{-1} (blue) and 20 deg s^{-1} (red) stimuli; data averaged across all subjects.

Table 3. Slope and R^2 values associated with the regression analysis of head-free eye-in-head velocity *versus* head velocity (*A*) and head-fixed eye velocity or head-free eye-in-head velocity *versus* head velocity alone (*B*)

		A. Eye-in-head *vs.* head (K_V) and head-fixed eye (K_{fx})				*B*. Eye-in-head *vs.* head (K_v)	
Condition	Subject	Slope (K_v)	Slope (K_{fx})	Delay (ms)	R^2	Slope (K_V)	R^2
IE	1	−0.702	0.635	25	0.997	−0.534	0.960
	2	−0.945	1.243	20	0.998	−0.610	0.967
	3	−1.035	1.068	5	0.985	−0.576	0.893
	4	−0.672	0.476	10	0.982	−0.557	0.932
	5	−1.029	1.109	5	0.991	−0.557	0.970
	6	−0.775	1.381	15	0.952	−0.592	0.909
SRE	1	−0.614	0.719	25	0.984	−0.556	0.628
	2	−1.004	1.186	5	0.997	−0.684	0.851
	3	−0.753	1.098	20	0.935	−0.501	0.516
	4	−0.887	1.266	15	0.955	−0.436	0.530
	5	−0.802	1.185	5	0.991	−0.598	0.611
	6	−0.702	0.585	25	0.935	−0.699	0.800
MRE	1	−0.618	0.666	5	0.979	−0.503	0.813
	2	−1.074	1.195	15	0.994	−0.606	0.858
	3	−1.045	1.508	15	0.905	−0.293	0.142
	4	−1.186	1.378	25	0.965	−0.508	0.582
	5	−0.793	1.106	15	0.959	−0.555	0.523
	6	−0.625	0.507	5	0.900	−0.587	0.676
IE	Average	−0.860	0.985	15	0.984	−0.571	0.938
SRE	Average	−0.794	1.006	15	0.966	−0.579	0.656
MRE	Average	−0.890	1.060	15	0.950	−0.509	0.599

The analysis shows that there is a much better fit to the data when a component proportional to head-fixed eye velocity is included (cf. R^2 values in columns 6 and 8). Optimum delays are also given (column 5). Data for 10 and 20 deg s^{-1} stimuli were combined in each subject.

Figure 8 shows examples obtained 600 ms after onset, near the time of peak head velocity, for the IE condition. Each data point represents a single response, with a different colour for each target velocity. Similar plots were obtained for the SRE and MRE conditions and linear regressions revealed a significant relationship between gaze and head velocity in all test conditions for all subjects (mean slopes: IE: 0.335, MRE: 0.344, SRE: 0.244; $P < 0.001$). In fact, even within each target velocity, many of the correlations between gaze and head velocity were significant when there was sufficient variability in head velocity. Out of 24 examples (4 velocities × 6 subjects), 13 correlations in the IE condition were significant ($P < 0.05$). Similarly, significant correlations were found at other times during target extinction (400 and 500 ms), but with differing slopes (mean for the IE condition 0.258 at 400 ms, 0.293 at 500 ms, 0.429 at 700 ms). In seeking evidence of a link between gaze and head velocity it has been assumed that gaze and head velocity are independent, but analysis from the previous section shows that when VOR gain (Kv) is <1 a proportion ($1 - K_V$) of head velocity contributes to gaze velocity. This contribution has been plotted in Fig. 8, where it is evident from its relatively low slope in most subjects that it cannot, by itself, account for the increased gaze velocity in those subjects.

The intra-subject variance of head velocity (measured at 600 ms) was significantly greater than the variance of head-free gaze velocity (Fig. 9*A*), suggesting that there was more error in translation of the estimate into head movement than gaze movement. However, normalisation of gaze and head velocity variance with respect to mean gaze or head velocity, respectively, for each target velocity revealed a distribution that was remarkably similar across target velocities (Fig. 9*B*) and was also similar for gaze (Fig. 9*C*) and head velocity (Fig. 9*D*) in all test conditions. The notable exception was that in the Control condition, gaze velocity exhibited a much smaller variance than for other test conditions because of the effects of visual feedback, although the head velocity distribution remained similar to the other test conditions. Importantly, the intra-subject variance in head-free gaze velocity (at 600 ms) was not significantly different to that of head-fixed gaze velocity, reinforcing the notion that gaze velocity is the primary controlled variable, as would be expected from the nature of the task. In contrast, the corresponding head velocity variance was 2–3 times greater.

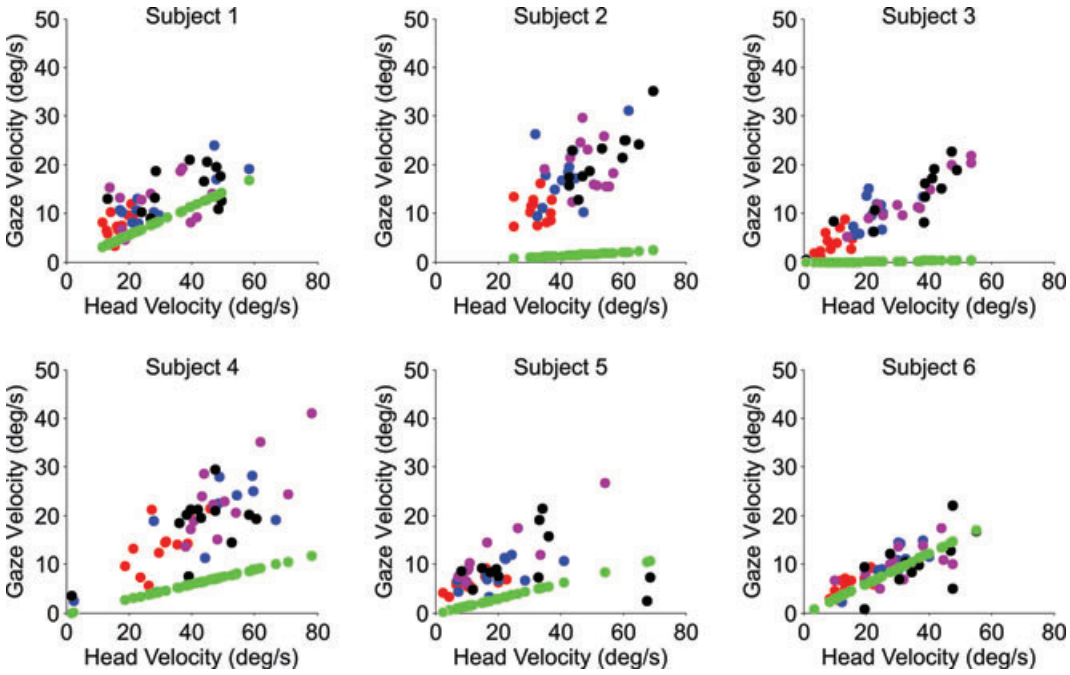

Figure 8. Gaze velocity 600 ms after target motion onset plotted against head velocity
Gaze velocity 600 ms after target motion onset plotted against head velocity in the head-free protocol for the initial extinction (IE) condition for each subject at all target velocities (10 deg s^{-1} (red), 20 deg s^{-1} (blue), 30 deg s^{-1} (purple), 40 deg s^{-1} (black)). Green circles indicate contribution to gaze velocity predicted by non-unity gain VOR.

Discussion

These experiments were designed to segregate the retinal and extra-retinal components of head-free pursuit, to identify their differing dynamic characteristics and to investigate interactions with the vestibulo-ocular reflex. Findings demonstrate that during head-free pursuit, human subjects are able to extract and temporarily store motion information after brief presentation of randomised target motion and use it both to initiate a visually driven eye movement response and to sustain appropriately scaled gaze and head movements during prolonged target extinction. The ability to sustain gaze velocity to an unseen target is a manifestation of

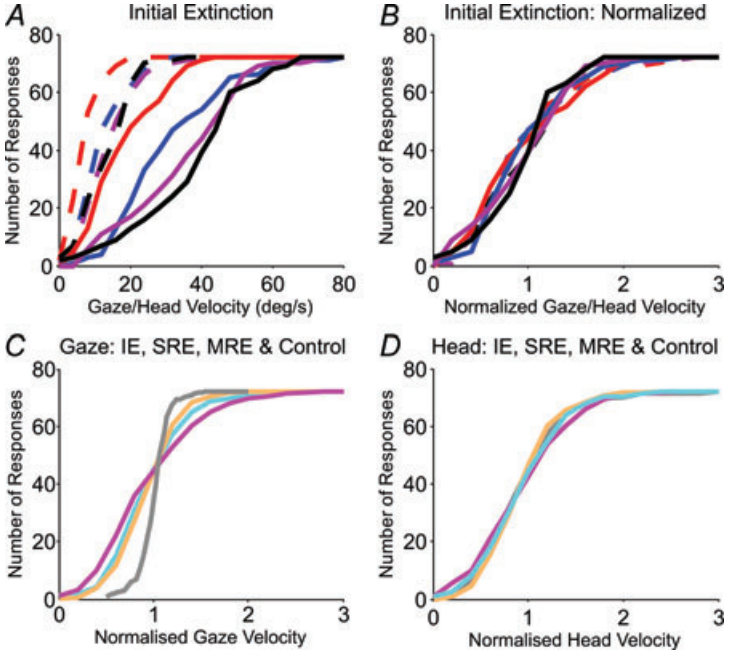

Figure 9. Gaze and head velocity distributions at 600 ms
A, cumulative distribution of gaze (dashed lines) and head (continuous lines) velocity for each target velocity (10 deg s^{-1} (red), 20 deg s^{-1} (blue), 30 deg s^{-1} (purple) and 40 deg s^{-1}(black)). *B*, data in *A* normalised to the mean gaze or head velocity and plotted against gaze or head velocity, respectively. Lower panels show a comparison of the normalised cumulative distribution of gaze velocity (*C*) and head velocity (*D*) for all test conditions: IE (magenta), SRE (cyan), MRE (orange) and Control (grey).

internal drive (pursuit maintenance) mechanisms and is dependent on expectation of target reappearance as found previously for similar head-fixed conditions (Barnes & Collins, 2008*a*,*b*). Most importantly, these results demonstrate that the internal drive component can be isolated by effectively splitting the MRE condition into two parts (SRE–IE pair), separated by fixation.

The IE condition evoked an anticipatory gaze velocity response prior to target appearance that increased much more slowly over time than the visually driven response. It was scaled to target velocity, suggesting that stored information from the first part (SRE) had been used to control the second part (IE) of each pair, even though successive pairs were randomised in speed and direction. Similar response trajectories were found under head-free and head-fixed conditions, although gaze velocity was less in the latter for comparable target velocities. It should be emphasised that the subjects were not trained in any sense to perform these tasks. The specific test conditions are ones that have previously been found to facilitate the generation of the extra-retinal pursuit component (Collins & Barnes, 2006). The IE condition responses were similar to head-fixed responses previously evoked by several repetitions of identical initial extinction stimuli (Barnes & Collins, 2008*b*). Although, the new method used here shows that multiple repetitions are not necessary to elicit the internally driven response, the scaling of this response was not as effective as previously found; there was little difference in the responses to the two highest velocity stimuli in either the head-fixed or head-free conditions.

In the head-free pursuit condition, initial sampling of target velocity also governed the control of average head velocity. Like gaze velocity, head velocity was scaled to target velocity in the absence of visual feedback. However, head velocity over the initial 750 ms from stimulus onset was similar irrespective of whether the target was briefly presented at the start (SRE and MRE), continuously present (Control) or completely absent (IE). In contrast, gaze velocity throughout the initial 750 ms was very different between test conditions (Fig. 7), since it was heavily influenced by visual feedback in the Control, MRE and SRE responses and by expectancy in the MRE, SRE and IE responses. The similarity of head movement for conditions in which the initial visual motion was either present (SRE, MRE and Control) or absent (IE) suggests that the visual input makes no direct contribution to head movement, but rather that its drive emanates solely from an internal source (see model, Fig. 6). The finding that there was considerable variance in both head and gaze velocity suggests that the internal drive for both represents an estimate of the required gaze or head velocity, rather than a precise control. This estimate exhibits the important property observed in magnitude estimation tasks, where variance is proportional to the magnitude of the estimate (Weber, 1850). The supposition of a common internal source for gaze and head velocity drive is supported by the finding of significant covariance between head and gaze velocity during target extinction. This should not, however, be taken to indicate that head and gaze are rigidly coupled, rather that they are fed by a common estimate of required velocity that is translated into differing velocity trajectories by dissimilar dynamics. Although head and gaze movements can be dissociated (Collins & Barnes, 1999), this probably occurs only when target movements are predictable, not randomised.

Comparison of pursuit with and without head rotation revealed that, under all extinction conditions, head rotation in the same direction as the target evoked higher-velocity tracking of the unseen target than with head fixed. Detailed examination of head and eye movement during extinction indicated that the increase in gaze velocity with the head free was specifically related to head movement onset and was thus most probably associated with the VOR. The principal reason for the difference is revealed by eqn (3): gaze velocity is only equivalent in head-fixed and head-free conditions in the absence of any visual input if the gain of the VOR is exactly unity. The observed increases in head-free conditions resulted from a VOR gain that was slightly less than unity, but no lower than typically recorded during head rotation in darkness (Barnes, 1993). The small difference in pursuit gain between head-fixed and head-free conditions accords with previous observations in which the target was continuously visible (Barnes, 1993), although the differences are more effectively revealed by the current test conditions since there was no influence of visual feedback. Some evidence indicates that the VOR is reduced to much lower levels during active head movements, but the majority has come from examination of gaze velocity during saccadic gaze shifts (e.g. Lefèvre *et al.* 1992; Roy & Cullen, 1998, 2004). In general, these studies show that VOR gain returns to normal towards the end of the gaze saccade, so it is possible that the effect is restricted to saccadic activity and does not impinge on smooth movements, as we find.

Humans are certainly able to use non-visual mechanisms to suppress VOR slow-phase responses if they imagine the presence of a head-fixed target in darkness (Barr *et al.* 1976; Barnes & Eason, 1988). The extra-retinal component of pursuit is a possible candidate for achieving this suppression but, if so, its association with anticipatory smooth pursuit (Barnes & Collins, 2008*b*) suggests it should be more effective in predictable than randomised conditions. Previously, Barnes & Eason (1988) found evidence that would support this, whereas McKinley & Petersen (1985) found evidence to the contrary. Recordings from vestibular neurons during various combinations of active and passive eye–head–body movements (McCrea *et al.* 1999; Cullen *et al.* 2001; Meng *et al.* 2005; Marlinski & McCrea,

2009) have demonstrated potential neuronal mechanisms for extra-retinal suppression of vestibular afferents, but some of this activity may influence principally the vestibulo-collic reflex (Roy & Cullen, 2003).

We have attempted to represent our major findings in the form of a model (Fig. 6), the basic components of which have previously been used to simulate the dynamic characteristics of head-fixed responses to the MRE and IE test conditions (Barnes & Collins, 2008*b*). Many of the interacting pathways and structures can be identified as indicated in Fig. 6. Of relevance to the current experiment is evidence that activity in the visual motion-sensitive medial superior temporal (MST) area is similar during both head-fixed and head-free pursuit (Ilg & Thier, 2003). This may therefore be the site at which the internal representation of target velocity in space (T') is encoded. MST is in bi-directional contact with the frontal eye fields (FEF) and supplementary eye fields (SEF), and activity in the FEF is related to gaze velocity during pursuit and VOR suppression (Fukushima *et al.* 2000, 2009; Akao *et al.* 2007, 2009; Fujiwara *et al.* 2009). The FEF and SEF are likely candidates for determining the expectation-dependent pursuit strategy to be used (Heinen & Liu, 1997; de Hemptinne *et al.* 2008), which is represented within the variable gain output (β) of internal drive (Fig. 6). It is likely that the output from FEF contains both visual and non-visual components of pursuit that interact with the VOR in the brainstem to control eye movement (Roy & Cullen, 2003; Ono & Mustari, 2009; Suzuki *et al.* 2009).

References

Akao T, Kurkin S, Fukushima J & Fukushima K (2009). Otolith inputs to pursuit neurons in the frontal eye fields of alert monkeys. *Exp Brain Res* **193**, 455–466.

Akao T, Saito H, Fukushima J, Kurkin S & Fukushima K (2007). Latency of vestibular responses of pursuit neurons in the caudal frontal eye fields to whole body rotation. *Exp Brain Res* **177**, 400–410.

Barnes GR (1993). Visual-vestibular interaction in the control of head and eye movement: the role of visual feedback and predictive mechanisms. *Prog Neurobiol* **41**, 435–472.

Barnes GR, Barnes DM & Chakraborti SR (2000). Ocular pursuit responses to repeated, single-cycle sinusoids reveal behavior compatible with predictive pursuit. *J Neurophysiol* **84**, 2340–2355.

Barnes GR, Benson AJ & Prior ARJ (1978). Visual-vestibular interaction in the control of eye movement. *Aviat Space Environ Med* **49**, 557–564.

Barnes GR & Collins CJ (2008*a*). The influence of briefly presented randomized target motion on the extraretinal component of ocular pursuit. *J Neurophysiol* **99**, 831–842.

Barnes GR & Collins CJ (2008*b*). Evidence for a link between the extra-retinal component of random-onset pursuit and the anticipatory pursuit of predictable object motion. *J Neurophysiol* **100**, 1135–1146.

Barnes GR & Eason RD (1988). Effects of visual and non-visual mechanisms on the vestibulo-ocular reflex during pseudo-random head movements in man. *J Physiol* **395**, 383–400.

Barnes GR, Grealy MA & Collins S (1997). Volitional control of anticipatory ocular smooth pursuit after viewing, but not pursuing, a moving target: evidence for a re-afferent velocity store. *Exp Brain Res* **116**, 445–455.

Barr CC, Scultheis LW & Robinson DA (1976). Voluntary, non-visual control of the vestibulo-ocular reflex. *Acta Otolaryngol* **81**, 365–375.

Becker W & Fuchs AF (1985). Prediction in the oculomotor system: smooth pursuit during transient disappearance of a visual target. *Exp Brain Res* **57**, 562–575.

Bennett SJ & Barnes GR (2003). Human ocular pursuit during the transient disappearance of a visual target. *J Neurophysiol* **90**, 2504–2520.

Bennett SJ & Barnes GR (2004) Predictive smooth ocular pursuit during the transient disappearance of a visual target. *J Neurophysiol* **92**, 578–590.

Burke MR & Barnes GR (2008). Anticipatory eye movements evoked after active following versus passive observation of a predictable motion stimulus. *Brain Res* **1245**, 74–81.

Carl JR & Gellman RS (1987). Human smooth pursuit: stimulus-dependent responses. *J Neurophysiol* **57**, 1446–1463.

Collewijn H & Smeets JB (2000). Early components of the human vestibulo-ocular response to head rotation: latency and gain. *J Neurophysiol* **84**, 376–389.

Collins CJ & Barnes GR (1999). Independent control of head and gaze movements during head-free pursuit in humans. *J Physiol* **515**, 299–314.

Collins CJS & Barnes GR (2006). The occluded onset pursuit paradigm: prolonging anticipatory smooth pursuit in the absence of visual feedback. *Exp Brain Res* **175**, 11–20.

Cullen KE, Roy JE & Sylvestre PA (2001). Signal processing by vestibular nuclei neurons is dependent on the current behavioral goal. *Ann N Y Acad Sci* **942**, 345–363.

de Hemptinne C, Lefèvre P & Missal M (2008). Neuronal bases of directional expectation and anticipatory pursuit. *J Neurosci* **28**, 4298–4310.

Fujiwara K, Akao T, Kurkin S & Fukushima K (2009). Discharge of pursuit neurons in the caudal part of the frontal eye fields during cross-axis vestibular-pursuit training in monkeys. *Exp Brain Res* **195**, 229–240.

Fukushima K, Kasahara S, Akao T, Kurkin S, Fukushima J & Peterson BW (2009). Eye-pursuit and reafferent head movement signals carried by pursuit neurons in the caudal part of the frontal eye fields during head-free pursuit. *Cereb Cortex* **19**, 263–275.

Fukushima K, Sato T, Fukushima J, Shinmei Y & Kaneko CR (2000). Activity of smooth pursuit-related neurons in the monkey periarcuate cortex during pursuit and passive whole-body rotation. *J Neurophysiol* **83**, 563–587.

Heinen SJ & Liu M (1997). Single-neuron activity in the dorsomedial frontal cortex during smooth-pursuit eye movements to predictable target motion. *Vis Neurosci* **14**, 853–865.

Ilg UJ & Thier P (2003). Visual tracking neurons in primate area MST are activated by smooth-pursuit eye movements of an "imaginary" target. *J Neurophysiol* **90**, 1489–1502.

Lefèvre P, Bottemanne I & Roucoux A (1992). Experimental study and modeling of vestibulo-ocular reflex modulation during large shifts of gaze in humans. *Exp Brain Res* **91**, 496–508.

Lisberger SG & Westbrook LE (1985). Properties of visual inputs that initiate horizontal smooth pursuit eye movements in monkeys. *J Neurosci* **5**, 1662–1673.

McCrea RA, Gdowski GT, Boyle R & Belton T (1999). Firing behavior of vestibular neurons during active and passive head movements: vestibulo-spinal and other non-eye-movement related neurons. *J Neurophysiol* **82**, 416–428.

McKinley PA & Peterson BW (1985). Voluntary modulation of the vestibuloocular reflex in humans and its relation to smooth pursuit. *Exp Brain Res* **60**, 454–464.

Marlinski V & McCrea RA (2009). Self-motion signals in vestibular nuclei neurons projecting to the thalamus in the alert squirrel monkey. *J Neurophysiol* **101**, 1730–1741.

Meng H, Green AM, Dickman JD & Angelaki DE (2005). Pursuit–vestibular interactions in brain stem neurons during rotation and translation. *J Neurophysiol* **93**, 3418–3433.

Ono S & Mustari MJ (2009). Smooth pursuit-related information processing in frontal eye field neurons that project to the NRTP. *Cereb Cortex* **9**, 1186–1197.

Rashbass C (1961). The relationship between saccadic and smooth tracking eye movements. *J Physiol* **159**, 326–338.

Robinson DA, Gordon JL & Gordon SE (1986). A model of the smooth pursuit eye movement system. *Biol Cybern* **55**, 43–57.

Roy JE & Cullen KE (1998). A neural correlate for vestibulo-ocular reflex suppression during voluntary eye-head gaze shifts. *Nat Neurosci* **1**, 404–410.

Roy JE & Cullen KE (2003). Brain stem pursuit pathways: dissociating visual, vestibular, and proprioceptive inputs during combined eye-head gaze tracking. *J Neurophysiol* **90**, 271–290.

Roy JE & Cullen KE (2004). Dissociating self-generated from passively applied head motion: neural mechanisms in the vestibular nuclei. *J Neurosci* **24**, 2102–2111.

Suzuki DA, Betelak KF & Yee RD (2009). Gaze pursuit responses in nucleus reticularis tegmenti pontis of head-unrestrained macaques. *J Neurophysiol* **101**, 460–473.

Weber EH (1850). Der Tastsinn und das Gemeingefuhl. In *Handworterbuch der Physiologie*, Vol. 3, Part 2, ed. R. Wagner, pp. 481–588. Vieweg, Braunschweig.

Author contributions

All experiments were performed in the Sensorimotor Neuroscience Laboratory in the Faculty of Life Sciences, University of Manchester, UK, headed by G.R.B. The conception and design of experiments was made by G.R.B.; R.A. collected the experimental data and drafted the paper. Both authors performed the data analysis and interpretation of the data. The revision of the manuscript was made by both authors and they also approved the final version of the manuscript.

Acknowledgements

This work was supported by the Medical Research Council, UK.